The Application of Multi-Photon Ionization Mass Spectrometry to the Study of the Reactions O + C_2H_4, F + C_3H_6, F + c-C_3H_6, F + CH_3OH, H + CH_2OH and O + CH_3O

P. Heinemann-Fiedler and K. Hoyermann

Institut für Physikalische Chemie der Universität Göttingen, Tammannstraße 6, D-3400 Göttingen

Chemical Kinetics / Mass Spectrometry / Multi-photon Processes

The experimental arrangement of a time-of-flight mass spectrometer with multi-photon ionization and electron impact ionization is described. This set up was combined with a discharge flow reactor and a molecular beam sampling device. The detection of the radicals CH_3, C_3H_5, CH_2OH and their deuterated analogs by the wave-length selective multi-photon ionization allowed the identification of primary products of elementary reactions in the gas-phase (around 1 mbar). The branching ratios for the reactions

$$O + C_2H_4 \rightarrow CH_3 + HCO$$

$$F + C_3H_6 \rightarrow CH_3 + C_2H_3F$$

$$F + c\text{-}C_3H_6 \rightarrow c\text{-}C_3H_5 + HF$$

were determined as (0.5 ± 0.15), (0.5 ± 0.1), (0.95 ± 0.05), respectively. – For the reactions of the CH_2OH and CH_3O radicals with H and O atoms, the following reaction paths were established:

$$CH_2OH/CH_3O + H \rightarrow CH_3 + OH \qquad (30\%)$$

$$CH_2OH + D \rightarrow CHDOH + H$$

$$CH_3O + O \rightarrow CH_3 + O_2 \qquad (>50\%).$$

1. Introduction

An enormous amount of interest has been shown in the elementary chemical reactions underlying such important gas-phase processes as pyrolysis, combustion of hydrocarbon and formation and destruction of air-pollutants.

Detailed experimental studies have been performed using different reactor types (e.g. static photolysis, discharge flow reactors, shock tubes), detection methods (e.g. absorption spectroscopy, LIF, LMR, gaschromatography, mass spectrometry) and sampling techniques (molecular beam, pin hole, cold trap). The method "discharge flow reactor/mass spectrometric detection" – the topic of this paper – has attracted special attention for obvious reasons: (i) simple production of atoms and radicals by microwave discharges and a good reaction time resolution by fast gas flows; (ii) a variety of sampling devices due to the stationary conditions in the reactor; (iii) mass spectrometry as a universal detection method. Mass spectrometry/electron impact ionization is widely used in the detection of molecules and radicals; fragmentation patterns of stable species allow the identification of isomers under specific experimental conditions, although the fragment ions can interfere with the detection of radicals present in the reaction mixture. Now a new method – the multi-photon ionization (MPI) by lasers at a radical specific wave-length – is experimentally available. (For a recent review see [1]). In this paper we want to describe an experimental arrangement which combines the advantages of a discharge flow reactor/molecular beam sampling, and mass spectrometric detection with electron impact ionization and multi-photon ionization of radicals. This arrangement has been applied to the study of primary products of elementary chemical reactions in the gas-phase.

2. Experimental

The experimental arrangement is shown in Figs. 1 and 2 in some detail.

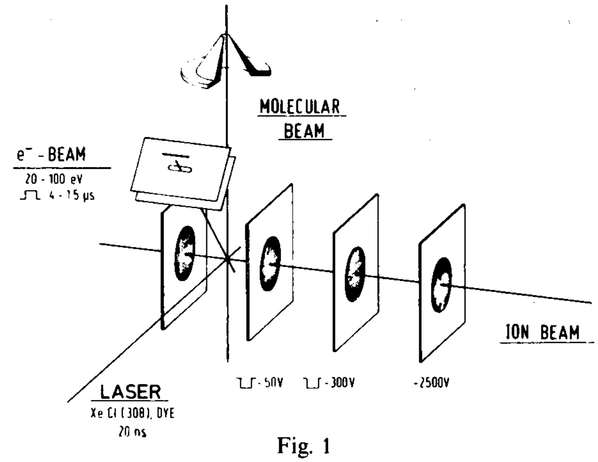

Fig. 1
Principle arrangement

Time-of-Flight (TOF)-Mass Spectrometer

The home-built time-of-flight mass spectrometer was designed on the principles of [2] and another realization of the Bendix type MA 2 with major modifications. It consists of the ion source, the ion extraction and drift tube, and the ion detection system. The ion source is formed by two parallel plates (3 cm × 3 cm, distance 0.8 cm) with Ni plated mesh (Buckbee-Mears Comp., MN 17.23 transmission 82.9%) at ground potential. The molecular beam is

Ber. Bunsenges. Phys. Chem. *92*, 1472–1477 (1988) – © VCH Verlagsgesellschaft mbH, D-6940 Weinheim, 1988.
0005–9021/88/1212–1472 $ 02.50/0

crossed at 90° by the laser beam in the center of the free volume. The dye laser (Lambda Physik FL 2002) is pumped by an excimer laser (Lambda Physik EMG 101) with a pulse duration of 20–25 ns and a repetition rate of up to 20 Hz. The laser is focussed into the ionization center by different lenses (*f* = 40, 100, 200, 400 mm) depending on the experimental conditions for detection. The electron gun for electron impact ionization (EI) (Rhenium wire 0.1 mm diameter, current 4–5 A) fires at 45° to the laser/molecular beam; the electron energy can be varied from 20 to 100 eV and the electron beam pulse is adjusted to a width of 0.5– 5 μs with a repetition rate up to 15 kHz. The electron emission is controlled automatically, via an electron trap current, by the filament current. Two magnets across the arrangement emission cathode/trapping anode assure a small effective ionization volume. The ions (both in MPI and EI mode) are extracted by applying short pulsed voltages across the plates (first stage: 0–100 V (0.5–5 μs), second stage: 0–300 V (0.5–5 μs)) and a constant main acceleration field (–1 kV to –3 kV). The voltages, the gate pulses and the delays are adjusted for maximum ion intensity and mass resolution. The drift tube (150 cm length) contains a cylinder of stainless steel mesh on the low negative potential of the last acceleration plate. Some electrostatic lenses focus the ion beam onto the detector. The low negative voltages are adjustable from voltage dividers of a high stability voltage supply (Fluke 415 B). The detector consists of two microchannel plates (Varian 8946, 25 mm diameter) separated by a 4 μm Cu foil and imbedded in a ceramic housing (Macor). Typical operation voltages (from a Nukletron 12508 voltage supply) are 0.8–1 kV per plate and a potential difference of 500 V from plate to anode.

After amplification by the detector (gain 10000), the voltage over a 50 Ω resistor is further enhanced by a fast amplifier (500 MHz, LeCroy, VV 100 B), the rise time is below 1 ns. The full time-of-flight mass spectrum is recorded by a fast transient digitizer (LeCroy SA 3500, 200 MHz), averaged over typically 100–10000 cycles and analyzed by a microcomputer/read out set up.

The operation of the mass spectrometer is easily switched from the EI to the MPI mode; in the MPI mode the trigger is set by the scattered light of the laser on a photomultiplier.

The oil free vacuum of 10^{-5} mbar in the ion source is maintained by turbo molecular pumps (single stage molecular beam sampling: 450 l/s Leybold; double stage, differential pumping: 150 l/s); the drift tube is evacuated independently ($< 10^{-6}$ mbar) by a 150 l/s turbo molecular pump.

Discharge-Flow-Reactor

The discharge-flow-reactor has been described previously (see for example [3]). Only the essentials are presented here (see Fig. 2). The atoms (F, O, H, D, N) are produced in F_2, O_2, H_2, D_2 and N_2 mixtures with He by a microwave discharge. Oxygen atoms free from molecular oxygen are favourably generated via the reaction $N + NO \rightarrow N_2 + O(^3P)$. The other reactant (hydrocarbon, NO) is diluted with inert gas and injected into the main gas flow. High flow velocities (up to 80 m/s) are maintained by a large rotary pump; the reaction times are varied by the flow velocity or by the distance between injection probe and sampling orifice.

Molecular Beam Sampling

The arrangement of the sampling nozzle and the skimmer is shown in Fig. 2 for the differentially pumped double stage set up. (Orifice diameter: 0.6 mm (nozzle), 1.0 mm skimmer). This arrangement is used at "high" pressures in the flow reactors (> 1.3 mbar), for low pressures a one stage expansion is feasible. The mounting is such that the flow reactor, the sampling nozzle, the skimmer and the ion source are aligned via sliding seals and bellows. The quality of the molecular beam (low divergence) and the position can be checked by sweeping the narrow laser beam through the molecular beam in the ion source and thereby measuring the concentration profile of the molecular beam.

Substances

The chemicals were of commercial grade. (He (99.996%), Ar (99.998%), N_2 (99.998%), O_2 (99.995%), H_2 (99.996%), D_2 (99.7%), F_2 (99%), CH_4 (99.99%), c-C_3H_6 (99.0%), C_3H_6 (99.0%), C_2H_4 (99.8%), CH_3OH (99.8%), CH_3OD (99.0%), CD_2HOH (98%), CD_3OD (99.0%), NO (99.0%)).

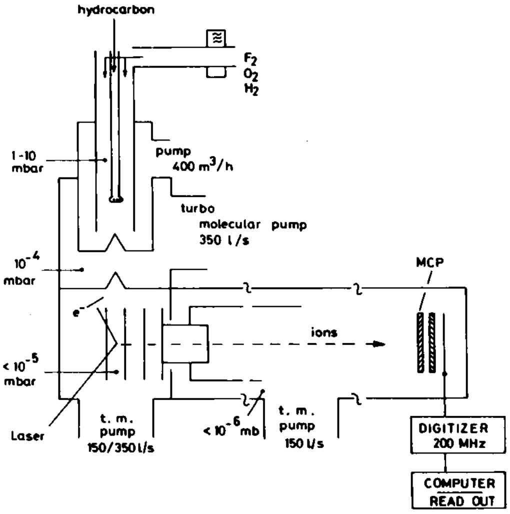

Fig. 2
Schematics of the experimental arrangement of the discharge flow reactor/molecular beam sampling/MPI-EI-TOF-mass spectrometer

Results and Discussion

1. Test of the Experimental Arrangement

The performance of the experimental arrangement is demonstrated in Fig. 3, where several original mass spectra are shown. In Fig. 3a the electron impact mass spectrum of C_3H_6 exhibits a good signal-to-noise ratio and an adequate mass resolution. In Fig. 3b the MPI mass spectra of the radicals CH_3, CH_2D, and CHD_2 are presented. The CH_3 radicals were produced by the reaction of F atoms with CH_4

$$CH_4 + F \rightarrow CH_3 + HF \qquad (1)$$

and the deuterated methyl radicals by the atom-radical reaction

$$D + CH_3 \rightarrow CH_2D + H \qquad (2a)$$

$$D + CH_2D \rightarrow CHD_2 + H. \qquad (2b)$$

(The MPI spectra of CH_3 and CD_3 have been described in detail by Hudgens et al. in a series of papers, see for e.g. [1, 4].) In our study the transition 3 d $^2E''O_0^0$ at $\lambda = 450.8$ nm for CH_3 was chosen, the corresponding transition of CD_3 is shifted to $\lambda = 451.3$ nm. The reactions (2a), (2b) are known to be fast [5].

Fig. 3b clearly indicates the detection of CH_3 radicals in the presence of high excess of CH_4 without fragment ion formation at *m*/*e* = 14, 13 and with a good signal-to-noise ratio. Good mass resolution is demonstrated in Fig. 3b2. The ion signals at the masses 15, 16, 17 do not correspond quantitatively to the CH_3, CH_2D, CHD_2 concentrations, as the absorption coefficients at the fixed absorption wavelength ($\lambda = 450.8$ nm) are different. The better mass resolution in the MPI experiment compared to electron impact ionization is explained by the smaller ion production volume and by the energy collimation [2].

The MPI mass spectrum of CH_3 may be compared to the EI mass spectrum at 100 eV, showing the different fragmentation pattern (the ratio of the ion signals at m/e = 15, 14 is $I(15)$: $I(14)$ = 47:100). However, it should be borne in mind that at a lower ionization energy the cracking is drastically reduced albeit with a large reduction in the total ion intensity. (For the fragment ion formation of CH_3 at m/e = 15, 14 as function of electron energy see [6]).

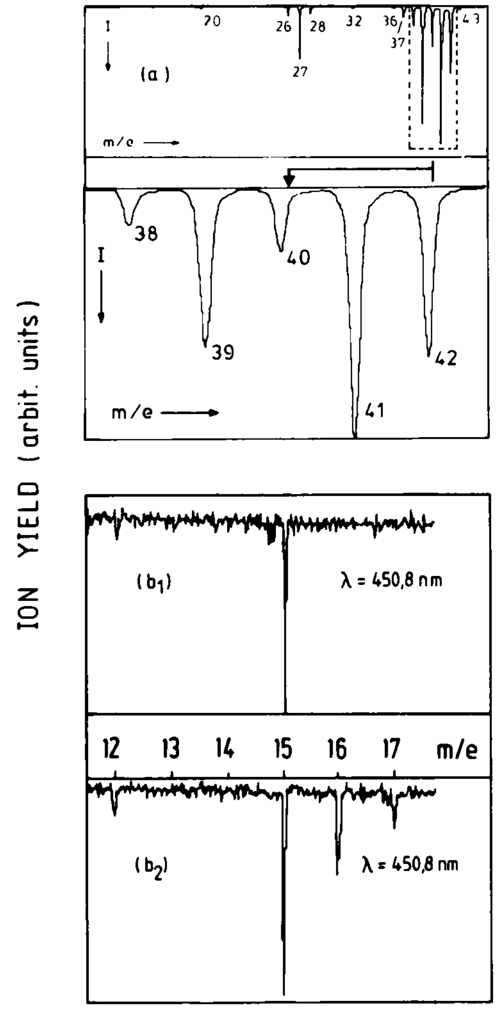

Fig. 3

(a) Mass spectrum (electron impact ionization) of propene demonstrating the mass resolution of the TOF mass spectrometer

(b) Mass spectra of CH_3 radicals

- (b1) Detection of the CH_3 radical by MPI at $\lambda = 450.8$ nm (dye: Coumarin 2; 6 mJ laser energy; averaged signal from 500 laser shots; CH_3 concentration in the flow reactor: $3 \cdot 10^{-4}$ mbar; background pressure in the ion source: $6 \cdot 10^{-6}$ mbar $[CH_4]_0/[CH_3] = 50$)
- (b2) MPI mass spectrum at $\lambda = 450.8$ nm Addition of D atom: $CH_3 + D \rightarrow CH_2D + H$, $CH_2D + D \rightarrow CHD_2 + H$ (conditions as in (b1))

2. Primary Products of the Reaction O + C_2H_4

The primary products and branching ratio of the different reaction channels of the reaction O + C_2H_4 have been discussed in the literature (see [7–14]):

$$O + C_2H_4 \rightarrow CH_3 + HCO \tag{3a}$$

$$\rightarrow C_2H_3O + H \tag{b}$$

$$\rightarrow CH_2CO + H_2\,. \tag{c}$$

The reaction (3) is slow at room temperature ($k_3 = 4.5 \times 10^{11}$ cm³/mol s, see [15]), whereas the secondary radical reactions

$$O + CH_3 \rightarrow HCHO + H \tag{4}$$

$$O + HCO \rightarrow CO_2 + H \tag{5}$$

$$\rightarrow CO + OH$$

are fast [15, 16] ($k_4 = 8.4 \times 10^{13}$ cm³/mol s, $k_5 = 3 \times 10^{13}$ cm³/mol s).

This complicates a direct absolute determination of the branching ratio.

At high excess of C_2H_4 ($[C_2H_4]_0/[O]_0 > 500$) secondary radical consuming reactions like (4), (5) are suppresed. Under these experimental conditions CH_3 radicals were detected by MPI. An absolute calibration of the amount of CH_3 formed with the amount of C_2H_4 consumed was not possible for these initial concentration ratios. At lower excess of C_2H_4 ($[C_2H_4]_0/[O]_0 = 10-50$), however, the ratio $\Delta[CH_3]/\Delta[C_2H_4] \geqslant 0.37$ was determined. The procedure involved determining the relative EI mass spectrometric sensitivity of C_2H_4 and CH_4 and the MPI sensitivity of CH_3 with respect to the EI sensitivity of $\Delta[CH_4]$ (see reaction (1)). The value of $k(3a)/k_{total} \geqslant 0.37$ is a lower limit as CH_3 radicals are consumed via reaction (4). From the mass spectrometric measurement (EI) of HCHO and the numerical simulation of the full reaction scheme (reaction (3), (4), (5)) the ratio $k(3a)/k_{total} \approx 0.5 \pm 0.15$ is deduced. (The error margin stems from the uncertainties of the successive calibration procedures.)

The value of $k(3a)/k(3) \approx 0.5$ lies within the values reported so far [7–14] (0.95; 0.95; 0; 0.64; 0.44; 0.21; 0.73; 0.5).

3. Primary Products of the Reactions F + C_3H_6 and F + c-C_3H_6

The primary products of the reaction F + propene have been identified by EI and MPI mass spectrometry resulting in the following reaction scheme:

$$F + C_3H_6 \rightarrow C_3H_5 + HF \tag{6a}$$

$$\rightarrow C_2H_3F + CH_3 \tag{6b}$$

$$\rightarrow C_3H_5F + H\,. \tag{6c}$$

The methyl radical CH_3 has been identified by its MPI spectrum at $\lambda = 450.8$ nm and the allyl radical C_3H_5 by its MPI spectrum at $\lambda = 498.5$ nm. These are the absorption wavelengths already reported by Hudgens et al. [1, 17], who analyzed the spectra in detail. By calibration procedures (F + CH_4, reaction (1)) route (6b) was found to contribute 50 ± 5% to the total reaction. Route (6c) is a minor route (10%), as estimated from the EI mass spectrum of C_3H_5F, leading to a contribution of around 40% for route (6a).

The reaction of F atoms with cyclopropane (the isomer of propene) has been studied previously [18] and found to be fast, too. In that study, the main reaction has been identified as

$$F + c\text{-}C_3H_6 \rightarrow c\text{-}C_3H_5 + HF\,. \qquad (7)$$

An isomerization reaction of the radical

$$c\text{-}C_3H_5 \rightarrow C_3H_5 \qquad (8)$$

has been neglected, as the recombination product of c-C_3H_5, bi-cyclopropane, was detected. However, in the MPI study of reaction (7) small signals at mass $m/e = 41$ were detected, as shown in Fig. 4b$_1$. A calibration routine using reaction (6a) as a standard yields a contribution of the allyl radical in reactions (7) and (8) of around 5%. The proof that c-C_3H_5 is the main product of reaction (7) was established by the reactions of the C_3H_5 radical with hydrogen and deuterium atoms.

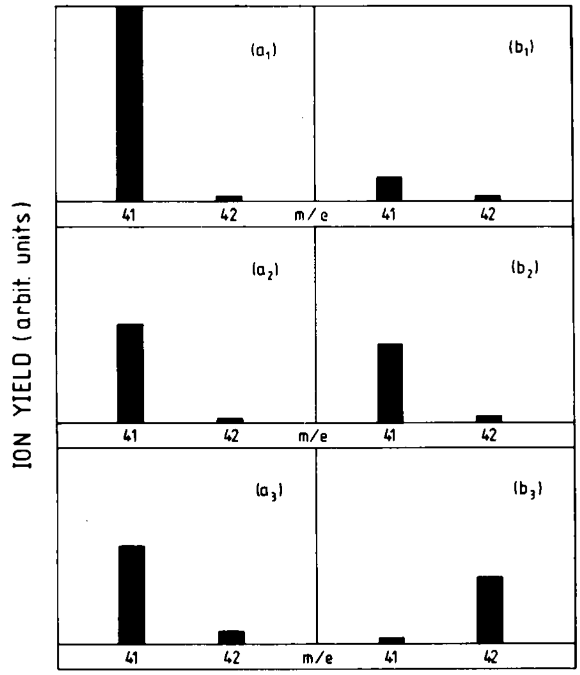

Fig. 4
The detection of C_3H_5 radicals by MPI (Production of C_3H_5 radicals via reaction (6a): $C_3H_6 + F \rightarrow C_3H_5 + HF$; $\lambda = 498.5$ nm; dye: Coumarin 307; 7 mJ laser energy; 500 laser shots)

(a$_1$) C_3H_5 concentration in the reactor : $2 \cdot 10^{-4}$ mb
(a$_2$) addition of H atoms
(a$_3$) addition of D atoms
(b$_1$) Reaction (7): c-C_3H_6 + F → c-C_3H_5 + HF (wave-length $\lambda = 498.5$ nm)
(b$_2$) addition of H atoms (detection wave-length as c$_1$)
(b$_3$) addition of D atoms (see text)

According to the study [18], the following reaction schemes hold at pressures of around 1 mbar

$$C_3H_5 + H \xrightarrow{9a} C_3H_6^* \xrightarrow[M]{} C_3H_6 \qquad (9b)$$

$$\longrightarrow C_2H_3 + CH_3 \qquad (9c)$$

$$c\text{-}C_3H_5 + H \longrightarrow c\text{-}C_3H_6^* \qquad (10a)$$

$$\downarrow$$

$$C_3H_6^* \xrightarrow{M} C_3H_6 \qquad (10b)$$

$$\longrightarrow C_3H_5 + H \qquad (10c)$$

$$\longrightarrow C_2H_3 + CH_3$$

The MPI measurements, presented in Fig. 4, support these mechanisms. As seen from Fig. 4a$_1$ and a$_2$, H atoms remove C_3H_5 radicals by the reactions (9a), (9b); the isotope exchange reaction

$$C_3H_5 + D \rightarrow C_3H_4D + H \qquad (9a-D)$$

is a minor channel, as seen from the low C_3H_4D signal at $m/e = 42$ in Fig. 4b$_3$.

From the reaction scheme (10), transformation of c-C_3H_5 radicals to C_3H_5 radicals by reaction with H atoms would be expected. This is demonstrated in Figs. 4b$_1$, b$_2$, where an increase in C_3H_5 radicals due to reaction of c-C_3H_5 with H atoms is observed; the radical isomerization reaction via (10a), (10b) and (10c) can be thought of as a titration reaction of c-C_3H_5 radicals. Using D atoms the corresponding reaction

$$c\text{-}C_3H_5 + D \rightarrow C_3H_4D + H \qquad (10c-D)$$

is observed as illustrated in Fig. 4b$_3$.

The low yield of allyl radicals in the reactions (7) and (8) is in some contradiction to [17], where the c-C_3H_5 isomerization reaction to C_3H_5 was suggested to be dominant.

4. The CH_2OH, CH_3O Radicals and their Reactions with H and O Atoms

The CH_2OH radical is an important radical in the oxidation and pyrolysis of the alternative fuel CH_3OH in combustion systems, as primary attack on CH_3OH by atoms and radicals yields CH_2OH. Since the sensitive detection of CH_2OH by MPI [1, 19] is known, new studies of the reactions of CH_2OH are possible. The specific wave-length selective detection of CH_2OH should considered in the light of the fact that in EI mass spectrometry the CH_2OH^+ ion is the dominant ion of all primary alcohols.

The reactions of F atoms with normal methanol CH_3OH and with the partially and fully deuterated methanols CH_3OD, CD_2HOH, CD_3OH, and CD_3OD have been studied with respect to the wave-length dependent ionization of the hydroxy methylene radicals:

$$F + CH_3OH \longrightarrow HF + CH_2OH \qquad (11a)$$

$$\longrightarrow HF + CH_3O \qquad (11b)$$

$$F + CH_3OD \longrightarrow HF + CH_2OD \qquad (12a)$$

$$\longrightarrow DF + CH_3O \qquad (12b)$$

$$F + CD_2HOH \longrightarrow DF + CDHOH \qquad (13a')$$

$$\longrightarrow HF + CD_2OH \qquad (13a'')$$

$$\longrightarrow HF + CD_2HO \qquad (13b)$$

$$F + CD_3OH \longrightarrow DF + CH_2OH \tag{14a}$$

$$\longrightarrow HF + CD_3O \tag{14b}$$

$$F + CD_3OD \longrightarrow DF + CD_2OD \tag{15a}$$

$$\longrightarrow DF + CD_3O \tag{15b}$$

The abstraction reaction both from the hydroxylic and aliphatic hydrogen with fluorine atoms and the branching ratios (a)/(b) have been studied independently as reported in a previous paper [20]. Figure 5 shows the MPI mass spectra of the different radicals, the wave-lengths employed and the precursor methanols. By isotopic labelling it is clearly demonstrated that a selective ionization of the hydroxymethylene radical is observed. For example the CHDOH and the CD_2OH radicals can be distinguished easily by switching the wavelength from 487.2 nm to 488.2 nm as illustrated in Fig. 5; the ion intensity is reversed from 2.7:1 to 1:16. In Fig. 6 a comparison between the EI mass spectra of various radical mixtures CH_2OH/CH_3O and the MPI mass spectra of the CH_2OH radicals is shown. The sensitive detection of the labelled CH_2OH radicals and of the CH_3 radicals permits questions concerning the specific details of the CH_2OH, CH_3O + H/D reactions to be answered, questions which were left open in a previous paper [21].

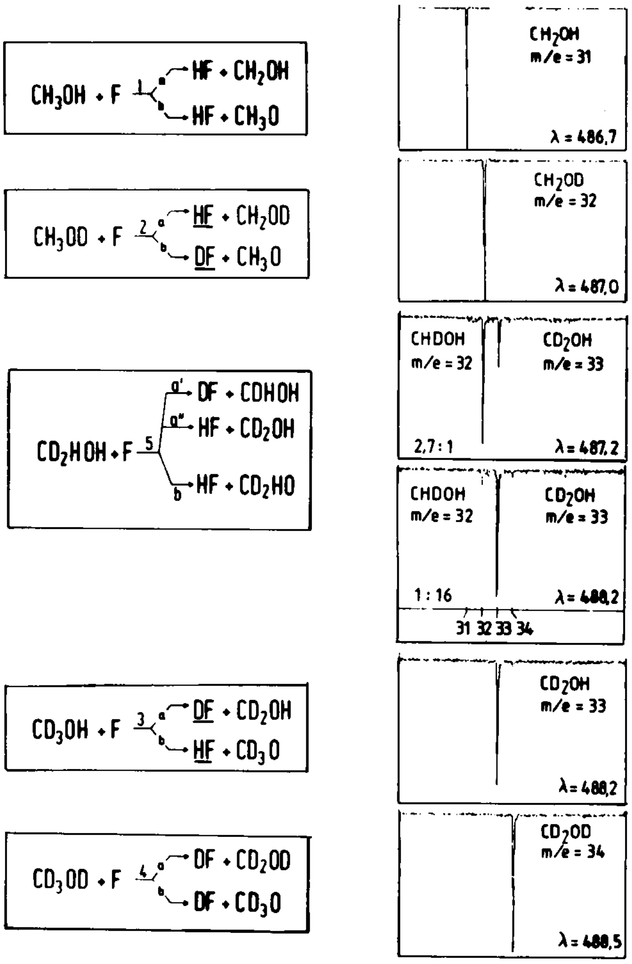

Fig. 5
The MPI mass spectra of the normal and deuterated hydroxy methylene radicals (wave-length λ as indicated; 100 laser shots)

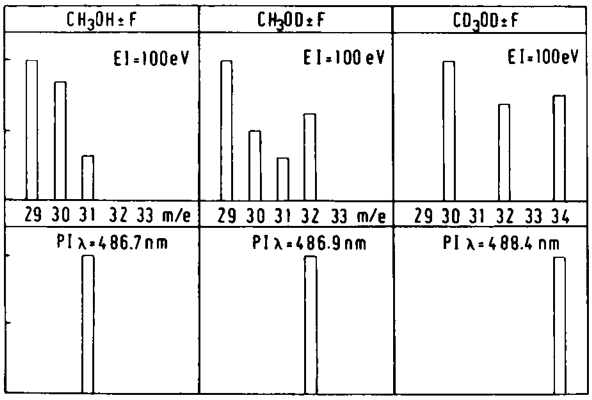

Fig. 6
Comparison between the EI (100 eV) and MPI mass spectra of the radical mixtures hydroxymethylene/methoxy radicals as produced in the given reactions

CH_2OH and CH_3O were prepared via reaction (11). The consumption of CH_2OH and the formation of CH_2OD was observed in the reaction of CH_2OH with D atoms:

$$\underline{CH_2OH} + D \longrightarrow \underline{CH_2OD} + H. \tag{16}$$

(The radicals detected by MPI are underlined.)

CD_3O and CD_2OD were produced via reaction (15). As the reaction

$$\underline{CD_2OD} + H \nrightarrow CD_2OH + D \tag{17}$$

is endothermic the non-detection of CD_2OH in the exothermic reaction

$$CD_3O + H \nrightarrow CD_2OH + D \tag{18}$$

shows that no CH_3O radical isomerization is present.

Following the radical production via (11) and (15), the reactions with D and H atoms result in methyl radical formation

$$\underline{CH_2OH} + D \longrightarrow \underline{CH_2D} + OH \tag{19}$$

$$CH_3O + D \longrightarrow \underline{CH_3} + OD \tag{20}$$

and

$$\underline{CD_2OD} + H \longrightarrow \underline{CD_2H} + OD \tag{21}$$

$$CD_3O + H \longrightarrow \underline{CD_3} + OH. \tag{22}$$

By calibration procedures the contributions of CH_3 formation from both reactions to the total reaction was found to be in the order of 30%. This is in agreement with the previous study where the main reaction route (abstraction)

$$CH_2OH + H \longrightarrow CH_2O + H_2 \tag{23}$$

$$CH_3O + H \longrightarrow CH_2O + H_2 \tag{24}$$

was determined to be 75%.

CH_2OD radicals were prepared as in reaction (12) and the subsequent reaction with H atoms

$$\begin{aligned} \underline{CH_2OD} + H &\longrightarrow \underline{CH_3} + OD \\ &\not\longrightarrow CH_2D + OH \end{aligned} \tag{25}$$

indicates that no internal hydrogen shift is present.

The reaction $CH_3O + O \rightarrow CH_3 + O_2$ has been studied separately, CH_3O and CH_2OD radicals being produced via reaction (12). The admixture of oxygen atoms yields CH_3 but no CH_2D radicals. This is explained by the reaction scheme

$$CH_3O + O \longrightarrow (CH_3O_2^{\ddagger}) \longrightarrow \underline{CH_3} + O_2 \tag{26a}$$

$$CH_2OD + O \not\longrightarrow CH_2D + O_2 .$$

By following the consumption of CH_3OD using EI and thereby knowing the CH_3O concentration, the CH_3 yield from reaction (26) has been determined to be >50%. If corrections for the consumption of CH_3 by O atoms are made (see 3.2, reaction (4)) this limit is shifted to 65% ± 10%. This is in good agreement with the measurements of Zellner et al. [22], who found for the competing channel (26b)

$$CH_3O + O \longrightarrow CH_2O + OH \tag{26b}$$

a contribution of 8 – 20%.

5. Concluding Remarks

The wave-length selective multi-photon ionization technique with mass spectrometric detection seems to be a powerful addition to the range of methods previously applied to the study of elementary gas-phase reactions. The method has distinct advantages when studying radicals which do not fluoresce (like CH_3, CH_2OH) or where mass interference from fragment ions is otherwise observed (e.g. in the EI mass spectrometric studies of CH_2OH in a high excess of CH_3OH).

The wave-length selectivity of MPI is limited to those species with narrow absorption wave-length bands like CH_3. But as has been observed in this laboratory [23] for the other alkyl radicals C_2H_5, C_3H_7, C_4H_9, C_5H_{11} and for CH_3CO, broad absorption bands around 405 nm are seen; therefore for species specific detection additional mass selection is required. In order to avoid fragmentation by higher laser energies, in general lower energies have to be applied ("soft ionization"). The requirement of soft ionization may prevent the potential application of MPI detection to many species. In such cases conventional EI mass spectrometry will continue to be used, it being the standard and generally applicable method. Thus is to be expected that most work will involve a complementary application of the two techniques – as was required for the calibration procedures of the present work.

The continued interest and encouragement of Prof. H. Gg. Wagner is gratefully acknowledged. Thanks are due to Dr. M. Bartels for his cooperation in this project.

We wish to thank the Deutsche Forschungsgemeinschaft (Sonderforschungsbereich 93 "Photochemie mit Lasern") and to the Fonds der Chemischen Industrie for financial support.

References

[1] J. W. Hudgens, in: Advances in Multi-photon Processes and Spectroscopy (ed. S. H. Lin), World Scientific, Singapore, 1987.

[2] W. C. Wiley and I. H. McLaren, Rev. Sci. Instr. *26*, 1150 (1955).

[3] K. Hoyermann, R. Sievert, and H. Gg. Wagner, Ber. Bunsenges. Phys. Chem. *85*, 149 (1981).

[4] J. W. Hudgens, T. G. DiGuiseppe, and M. C. Lin, J. Chem. Phys. *79*, 571 (1983); J. Chem. Phys. *76*, 3337 (1982).

[5] M. Brouard and M. J. Pilling, Chem. Phys. Lett. *129*, 439 (1986).

[6] P. Heinemann, R. Sievert-Hofmann, and K. Hoyermann, Twenty-First Symposium (Int.) on Cumbustion, p. 865, The Combustion Institute, 1986.

[7] J. R. Kanofsky, D. Lucas, and D. Gutman, Fourteenth Symposium (Int.) on Combustion, p. 285, The Combustion Institute, 1973.

[8] B. Blumenberg, K. Hoyermann, and R. Sievert, Sixteenth Symposium (Int.) on Combustion, p. 841, The Combustion Institute, 1977.

[9] R. J. Buss, R. J. Baseman, G. He, and Y. T. Lee, J. Photochem. *17*, 389 (1981).

[10] H. E. Hunziker, H. Kneppe, and H. R. Wendt, J. Photochem. *17*, 377 (1981).

[11] U. Bley, P. Dransfeld, B. Himme, M. Koch, F. Temps, and H. Gg. Wagner, submitted to the Twenty-Second Symposium (Int.) on Combustion, 1988.

[12] W. C. Sridharan and F. Kaufman, Chem. Phys. Lett. *102*, 45 (1983).

[13] J. F. Smalley, F. L. Nesbitt, and R. B. Klemm, J. Phys. Chem. *90*, 491 (1986).

[14] Y. Endo, S. Tsuchiya, C. Yamada, E. Hirota, and S. Koda, J. Chem. Phys. *85*, 4446 (1986).

[15] W. Tsang and R. F. Hampson, J. Phys. Chem. Ref. Data *15*, 1087 (1986).

[16] I. R. Slagle, D. Sarzyński, and D. Gutman, J. Phys. Chem. *91*, 4375 (1987).

[17] J. W. Hudgens and C. S. Dulcey, J. Phys. Chem. *89*, 1505 (1985).

[18] M. Bartels, P. Heinemann, and K. Hoyermann, Twentieth Symposium (Int.) on Combustion, p. 723, the Combustion Institute, 1984.

[19] C. S. Dulcey and J. W. Hudgens, J. Phys. Chem. *87*, 2296 (1983).

[20] T. Khatoon and K. Hoyermann, Ber. Bunsenges. Phys. Chem. *92*, 669 (1988).

[21] K. Hoyermann, N. S. Loftfield, R. Sievert, and H. Gg. Wagner, Eighteenth Symposium (Int.) on Cumbustion, p. 831, The Combustion Institute, 1981.

[22] F. Ewig, D. Rhäsa, and R. Zellner, Ber. Bunsenges. Phys. Chem. *91*, 708 (1987).

[23] J. Edelbüttel-Einhaus, to be published.

(Eingegangen am 14. März 1988,
endgültige Fassung am 5. Juli 1988)
E 6755